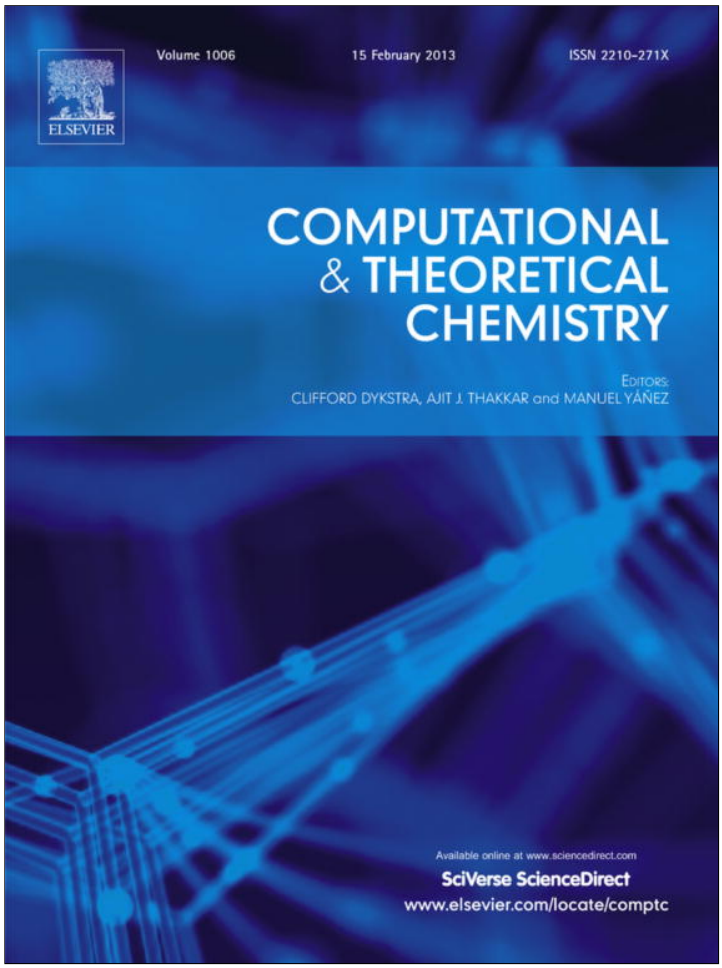

Computational and Theoretical Chemistry 1006 (2013) 37–46

Contents lists available at SciVerse ScienceDirect

Computational and Theoretical Chemistry

journal homepage: www.elsevier.com/locate/comptc

# Charge delocalization in *Z*-isomers of (4α → 6″, 2α → O → 1″)-phenylflavans with R = H, OH and $OCH_3$. Effects on bond dissociation enthalpies and ionization potentials

Rosana M. Lobayan [a,b,*,1], Erika N. Bentz [a,1], Alicia H. Jubert [c], Alicia B. Pomilio [d]

[a] Instituto de Investigaciones Científicas, Universidad de la Cuenca del Plata, Facultad de Ingeniería, Lavalle 50, 3400 Corrientes, Argentina
[b] Departamento de Física, Facultad de Ciencias Exactas y Naturales y Agrimensura, Universidad Nacional del Nordeste, Avda. Libertad 5300, 3400 Corrientes, Argentina
[c] CEQUINOR Facultad de Ciencias Exactas, Universidad Nacional de La Plata, CC 962, 1900 La Plata, Argentina
[d] IBIMOL (ex PRALIB) (UBA, CONICET), Facultad de Farmacia y Bioquímica, Universidad de Buenos Aires, Junín 956, C1113AAD Buenos Aires, Argentina

ARTICLE INFO

*Article history:*
Received 4 September 2012
Received in revised form 31 October 2012
Accepted 6 November 2012
Available online 7 December 2012

*Keywords:*
Ionization potentials
Proanthocyanidins
Density functional theory
Atoms in molecules
Natural Bond Orbital analysis
Bond dissociation enthalpies

ABSTRACT

The (2 → O → 1″)-bridged 4-phenylflavans comprise an interesting structure, included in natural antioxidants such as simple and dimeric A-type proanthocyanidins, catechins and condensed tannins. This work concerns the analysis of the stereoelectronic effects induced by substitution with R = H, OH and $OCH_3$ in Z-isomers of (4α → 6″, 2α → O → 1″)-phenylflavans using density functional methods in order to deepen the understanding of the molecular and structural properties of these compounds. A fully relaxed scan procedure was performed. A topological study of the molecular charge density (Bader theory, Atoms in Molecules) and a Natural Bond Orbital (NBO) analysis at the B3LYP/6-311++G** level were carried out. The stereochemistry of the molecules was discussed in detail focusing on the factors related to their antioxidant properties. Bond dissociation enthalpies (BDEs), ionization potentials (IPs) and electron affinities (EAs) were calculated for the lowest energy conformers. The Nuclear Magnetic Resonance (NMR) chemical shifts were also calculated at the B3LYP/6-31G** level, and compared with the earlier reported experimental values, showing that the thermodynamically most stable conformer is also the most stable kinetically. The effects of substituents on chemical shifts were quantified. Through a donor acceptor map a qualitative comparison among the studied compounds is given. The lower (higher) BDE (IP) values found for R = OH (4α → 6″, 2α → O → 1″)-phenylflavans, were explained herein by specific mechanisms of charge delocalization. These findings highlight the key role played by hyperconjugative interactions in the stereoelectronic effects induced by substitution as an important factor in understanding the associated values of BDEs and IPs.



## 1. Introduction

The family of flavonoids, including flavanones, dihydroflavonols (flavanonols), flavones, flavonols, isoflavones and catechins, has been identified as a major source of antioxidants in fruits, vegetables and beverages [1–3].

In the search for new antioxidants, flavan structures called our attention, as substructures of many important natural compounds, such as catechins (flavan-3-ols), simple and dimeric proanthocyanidins, and condensed tannins. These compounds are known as radical scavengers, for their redox properties and mechanisms of free radical interactions. Despite their structural diversity, these compounds as members of the large family of flavonoids share a common chemical feature of one or more phenolic groups, which operate as hydrogen or electron donors to inhibit reactive oxygen species (ROSs), such as singlet oxygen, superoxide, peroxyl radicals, and hydroxyl radicals [4–8].

These antioxidants are polyphenolic compounds that protect cells against the deleterious effects of ROS. An imbalance between antioxidants and ROSs results in oxidative stress, which has been associated with cancer, aging, atherosclerosis, ischemic injury, inflammation, tumors, and neurodegenerative diseases [8–10].

The (2 → O → 1″)-bridged 4-phenylflavans comprise an interesting structure, which is integrated into A-type proanthocyanidin molecules that have been synthesized as simple and dimeric molecules with various substituents on the aromatic rings [4].

To date there are no crystallographic reports on A-type proanthocyanidins, and only a few theoretical studies of their electronic, structural, and energetic properties. We have previously reported on the conformational space of unsubstituted and substituted 4-phenylflavans, and intramolecular bonding interactions related to their stability and reactivity [11–13]. The stereochemistry of the

* Corresponding author.
*E-mail addresses:* rlobayan@ucp.edu.ar, rmlb@exa.unne.edu.ar (R.M. Lobayan).
[1] These authors contributed equally to this work.

2210-271X/$ - see front matter © 2012 Elsevier B.V. All rights reserved.
http://dx.doi.org/10.1016/j.comptc.2012.11.008

molecules was also studied in our previous reports. The main substructure of the unsubstituted compound (**1**) is a [3.1.3]bicycle, consisting of two 6-membered rings, C and E, each involved in a benzo-γ-pyran, fused *via* a $CH_2$-3-containing bridge with C-2 and C-4 as bridgehead carbons (Fig. 1a). This bridge is a stereocenter that gives rise to *E* (*anti*)/*Z* (*syn*) isomers. The energy of the *E*-isomer is higher than that of *Z* due to the steric hindrance and high tension of the rings C and D [11]. The *Z*-isomer has both substituents Ph-2 and H-4 directed towards the same side of the plane of the molecule.

The present work focuses on the effect of substitution on the electronic distribution of (4α → 6″, 2α → O → 1″)-phenylflavan (**2** and **3**; Fig. 1a). The study of the role of the substituents on the properties of this set of *Z*-isomers of (4α → 6″, 2α → O → 1″)-phenylflavans was carried out in order to provide information on the relationship between the geometric structure and electronic charge delocalization.

Chemical bonds were studied and characterized using the theory of Atoms in Molecule (AIM), and also completed by a Natural Bond Orbital (NBO) analysis.

The bond dissociation enthalpies and ionization potentials for the lowest energy conformers were obtained in gas phase as good primary indices for free radical scavenging [14].

Nuclear magnetic resonance (NMR) parameters were also calculated, and compared with experimental values reported earlier [15]. The effect of substituents on them was also analyzed. An AIM/NBO study allowed us to rationalize experimental trends.

The relation between delocalization effects found in the phenylflavans substituted with R = OH and R = $OCH_3$ (**2** and **3**, respectively) led to the identification and quantification of the changes induced by substitution. Moreover, electron charge delocalization mechanisms associated with the enhancement of BDEs and IPs values are proposed herein.

This work is adding insight into the structure-radical scavenging activity relationship of flavans, through the knowledge of their antioxidant properties. The study in vacuum is relevant for measuring the intrinsic effects that will be useful for the quantification and understanding of the effects of different solvents on the reactivity of the molecules under study.

## 2. Methods

The lowest-energy conformers were studied by the density functional theory (DFT) as implemented by the Gaussian 03 package [16] using the Becke three-parameter hybrid functional combined with Lee–Yang-Parr correlation functional [17,18]. For geometry optimizations 6-31G** basis set was used for all atoms.

The main free radical scavenging mechanism of chain-breaking antioxidants (AHs) is a one-step H-atom transfer [19,20]:

$$AH + R^{\cdot} \rightarrow A^{\cdot} + RH \quad (1)$$

A higher stability of $A^{\cdot}$ accounts for a better efficiency of the antioxidant. In this case the reactivity of AH can be estimated using the calculated value of X-H (X = O, C; in R = OH and R = $OCH_3$, respectively) bond dissociation enthalpy (BDE). BDE is a main theoretical descriptor characterizing the free-radical scavenging activity of phenolic antioxidants [21]. The weaker the X-H bond, the easier the reaction of free-radical quenching (Eq. (1)). The values were calculated according to BDE = $H_r + H_h - H_p$, where $H_r$ is the enthalpy of the radical generated by H-abstraction, $H_h$ is the enthalpy of the H-atom (−0.499897 Hartree at this level of theory), and $H_p$ is the enthalpy of the parent molecule.

A second mechanism for free radical scavenging of chain-breaking antioxidants is a single-electron transfer (SET) (Eq. (2)) that can occur in parallel with the former one:

$$AH + R^{\cdot} \rightarrow R^{-} + AH^{\cdot +} \quad (2)$$

In this mechanism, the antioxidant transfers an electron to the free radical becoming a cation radical. The lower the ionization potential (IP), the easier is the electron abstraction. Adiabatic and vertical IP values were determined according to the equation IP = $E_{cr} - E_p$, where *p* and *cr* indicate the parent molecule and the corresponding cation radical generated after electron transfer. For adiabatic IP the Ecr structure was fully optimized, for vertical IP being necessary only a further single point calculation. In fact, vertical IP was calculated as the difference between the energy of the cation and the parent molecule, assuming that both have the ground-state nuclear configuration of the parent molecule. To assess reduction capacity, it was necessary to estimate the electron acceptance, which was possible by the calculation of vertical electron affinity (EA). Vertical EA was obtained as the difference between the energy of the parent molecule and the anion, calculated using the ground-state nuclear configuration of the parent molecule.

No spin contamination was found for radicals, the $\langle S^2 \rangle$ values being about 0.750 in all cases. Harmonic vibrational frequencies were computed at the same level (B3LYP/6-31G**) for both the parent molecule and radicals to characterize them as minima or

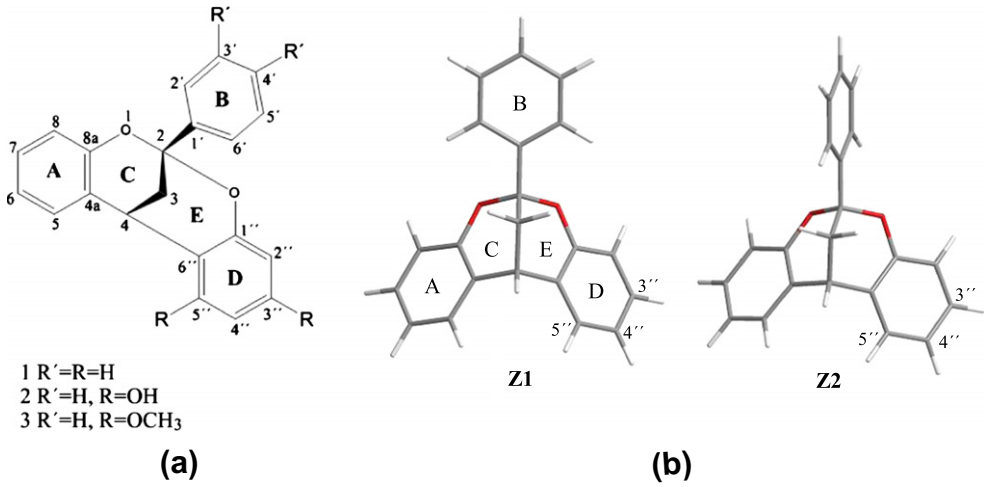


**Fig. 1.** Structures of (4α → 6″, 2α → O → 1″)-phenylflavans substituted with R = H, OH, $OCH_3$, (a) Geometry of the conformers of *Z*-isomer of (4α → 6″, 2α → O → 1″)-phenylflavans substituted with R′ = R = H at the B3LYP/6-31G** level of theory (b).

saddle points, and to evaluate the zero-point energy (ZPE) corrections to be included in all relative energies, bond dissociation energies, and ionization potentials. Single point energy (SPE) refinement was performed with a 6-311++G** basis set, and the relative energy and ionization potential 6-311++G** SPE values were then corrected by ZPE at B3LYP/6-31G** level.

Moreover, phenol was studied at the same level of calculation as a core for phenolics. Then, our calculations of BDEs and IPs were compared with phenol as reference.

The suitability of the selected level of calculation has been shown previously [14,17,19,22].

The isotropic $^{13}C$ magnetic shielding tensors of the lowest-energy conformers were calculated using the Gauge Including Atomic Orbital method implemented in G03 package at the B3LYP/6-31G** level of theory. The shielding tensors were converted to chemical shifts using TMS as reference. Calculated chemical shifts ($\delta$) were compared with NMR experimental values that had been recorded on a Bruker HFX 90 (90 MHz for $^{1}H$-NMR, 22.63 MHz for $^{13}C$-NMR) in $CDCl_3$ with tetramethylsilane (TMS) as internal reference [15].

The topological analysis and evaluation of local properties were performed by the PROAIM software [23] using the wave functions calculated at B3LYP and improved 6-311++G** basis set implemented in the G03 program. NBO analysis [24] was carried out in the same level.

## 3. Results and discussion

### 3.1. Structural features

The conformational space of the unsubstituted (4α → 6″, 2α → O → 1″)-phenylflavan (**1**) consisted of two low-energy conformers, e.g., Z1 and Z2 conformers (Fig. 1). The C-3–C-2–C-1′–C-6′ dihedral angle (orientation of ring B) showed the mean value of 88° for a set of structures that we called Z1 group, and about 0° for the Z2 group.

In contrast, substituted (4α → 6″, 2α → O → 1″)-phenylflavans showed eight conformers for R = OH (**2**), and four conformers for R = $OCH_3$ (**3**) (Fig. 2). The "T" and "C" subscripts refer to *anti* (*trans*) and *syn* (*cis*) configurations of H—O-3″ and H—O-5″ relative to the C-3″—C-4″ and C-5″—C-4″ bonds, respectively (Fig. 2). The mean values of the H—O-3″—C-3″—C-4″ and H—O-5″—C-5″—C-4″ dihedral angles were about 180° (*anti*) or near 0° (*syn*). The "CT" conformers were 0.79 kcal $mol^{-1}$ (0.91 kcal $mol^{-1}$) more stable than the "CC" for R = OH (R = $OCH_3$). Regardless of the substitution, Z1 conformers were on average 1.90 kcal $mol^{-1}$ more stable than the Z2, as we have previously reported [11,12].

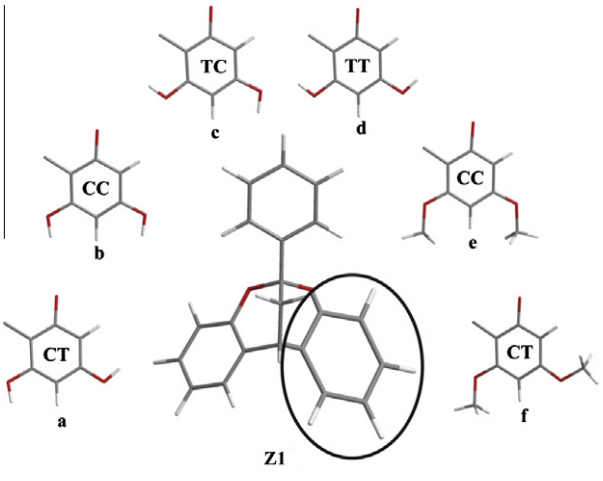


**Fig. 2.** Geometry of the conformers of Z1-isomer of (4α → 6″, 2α → O → 1″)-phenylflavans substituted with R′ = H, R = OH (a–d) and R′ = H, R = $OCH_3$ (e and f) at the B3LYP/6-31G** level of theory.

In this work, a fully relaxed scan procedure was performed (Figs. S1 and S2), showing that the C-2—C-1′ free rotation, which is involved in the rearrangement Z1–Z2, required about 2 kcal $mol^{-1}$ (Fig. S1′). Such low barrier suggested coexistence of the two types of conformers. However, the energy gap between Z1 and Z2 conformers led to 0.1–3.0% relative populations of the Z2 conformers at 298 K. For R = OH, 3.08%, 0.79%, 0.08% and 0.08% for $Z2_{CT}$, $Z2_{CC}$, $Z2_{TC}$ and $Z2_{TT}$, respectively. For R = $OCH_3$, 3.10% and 0.68% for $Z2_{CT}$ and $Z2_{CC}$, respectively.

The transition states for Z1 isomers of the substituted **2** and **3** found at the B3LYP/6-31G**/6-311++G** level of theory, and relative populations of the related lowest-energy conformers are shown in Table 1. When changing the C-3—C-2—C-1′—C-6′ torsion angle ($\tau$) from 0.0° to 360° in both substituted phenylflavans **2** and **3**, two transition states (TS), TS1 and TS2, were found (Table 1, Fig. S1′a and S1′b). Moreover, we came upon the $Z2_{CT}$ conformer for R = $OCH_3$ (**3**), which has not been previously found in the study of the conformational space by Molecular Dynamics [12].

Free rotation around C-3″—O-3″ and C-5″—O-5″ bonds that is involved in the CT-CC-TC-TT rearrangements, required about 3 kcal $mol^{-1}$ (Fig. S2′), which at 298 K accounted for a very small amount of energy. When changing the H-3″—O-3″—C-3″—C-4″ torsion angle ($\tau_1$) from 180.0° to 540.0°, two transition states were found, referring to CT and CC conformers (Table 1, Figs. S2′a and S2′e).

When changing the H-5″—O-5″—C-5″—C-4″ torsion angle ($\tau_2$) from 0.0° to 360.0°, two transition states were also found, referring to CC and TC conformers (Table 1, Fig. S2′b). Changing the H-3″—O-3″—C-3″—C-4″ torsion angle ($\tau_1$) from 0.0° to 360.0°, two transition states were also found, referring to TC and TT conformers (Table 1, Fig. S2′c). Changing the H-5″—O-5″—C-5″—C-4″ torsion angle ($\tau_2$) from 180.0° to 540.0°, two transition states were also found, referring to TT and CT conformers (Table 1, Fig. S2′d). TC and TT conformers were not found for R = $OCH_3$ (**3**) (Fig. S2′f).

### 3.2. Topology of the electron charge density function and NBO analysis

The chemical structures of molecules can be extracted from an analysis of the topology of the molecular charge density, $\rho(r)$, whose main features are summarized by the curvatures of $\rho(r)$ at critical points (CPs) [25].

The present article explores two types of CPs: (i) (3, -3) CP, which is a maximum in all directions, and all eigenvalues are negative. Since it often coincides with the position of the nucleus is called nuclear attractor or nuclear critical point (NCP), (ii) (3, -1) CP, which is a maximum in two directions, and a minimum in one of them, appearing at an intermediate point between two bonded atoms. For a system at equilibrium configuration it is called bond critical point (BCP).

If the Laplacian of $\rho(r)$ at a BCP is negative, the electron charge is locally concentrated at this point. This charge is provided as shared by both nuclei, and therefore, this is called *shared interaction* in the AIM theory. If, conversely, the Laplacian at BCP is positive, the electron charge is depleted on an infinitesimal area around BCP, which is the *closed shell interaction* in the AIM theory.

Another interesting parameter is the ellipticity, $\varepsilon$, which is $\lambda_1/\lambda_2 - 1$. The ellipticity is indicative of the similarity between perpendicular curvatures ($\lambda_1$ and $\lambda_2$) at BCP, and measures the degree to which density accumulates preferentially in a given plane containing the bond. If $\lambda_1 = \lambda_2$, then $\varepsilon = 0$, and the bond has cylindrical symmetry, such as the C–C single bond in ethane, and acetylene triple bond [25].

**Table 1**
Transition states for Z1 isomers of (4α → 6″, 2α → O → 1″)-phenylflavans substituted with R = OH, R′ = H and R = $OCH_3$, R′ = H found at B3LYP/6-31G**/6-311++G** level of theory. Relative populations of the related lowest energy conformers are also shown.[a]

| R | Conformer | Relative populations (%) | Transition state | Energies[b] (Hartree) | Dihedral scanned (Degrees) |
|---|---|---|---|---|---|
| OH | $Z1_{CT}$ | 72.58 | | | |
| | | | TS 2 | −1110.4675 | $\tau$ = 149.5° |
| | | | TS 1 | −1110.4677 | $\tau$ = 207.6° |
| | $Z2_{CT}$ | 3.08 | | | |
| $OCH_3$ | $Z1_{CT}$ | 79.19 | | | |
| | | | TS 2 | −1189.0203 | $\tau$ = 150.3° |
| | | | TS 1 | −1189.0204 | $\tau$ = 208.5° |
| | $Z2_{CT}$ | 3.11 | | | |
| OH | $Z1_{CT}$ | 72.58 | | | |
| | | | TS 1 | −1110.4651 | $\tau_1$ = 271.2° |
| | | | TS 2 | −1110.4647 | $\tau_1$ = 449.0° |
| | $Z1_{CC}$ | 19.03 | | | |
| | | | TS 1 | −1110.4644 | $\tau_2$ = 96.3° |
| | | | TS 2 | −1110.4656 | $\tau_2$ = 270° |
| | $Z1_{TC}$ | 2.23 | | | |
| | | | TS 1 | −1110.4620 | $\tau_1$ = 91.7° |
| | | | TS 2 | −1110.4616 | $\tau_1$ = 268.7° |
| | $Z1_{TT}$ | 2.12 | | | |
| | | | TS 1 | −1110.4659 | $\tau_2$ = 269.4° |
| | | | TS 2 | −1110.4646 | $\tau_2$ = 459.1° |
| $OCH_3$ | $Z1_{CT}$ | 79.19 | | | |
| | | | TS 1 | −1189.0189 | $\tau_1$ = 274.9° |
| | | | TS 2 | −1189.0186 | $\tau_1$ = 444.2° |
| | $Z1_{CC}$ | 17.02 | | | |

[a] Definition of dihedrals angles ($\tau$, $\tau_1$, and $\tau_2$) are given in the text.
[b] Energies corrected for zero point energy (ZPE).

The values of topological parameters, such as electronic charge density ($\rho_b$), Laplacian of charge density ($\nabla^2\rho_b$) and ellipticity ($\varepsilon$) at the BCPs for all chemical bonds of the lowest-energy conformers for **1**, **2** and **3** are shown as Supplementary material in Table S1. These topological parameters are shown for all structures, comprising the conformational space for R = OH (**2**), and R = $OCH_3$ (**3**) in Tables S2 and S3, respectively.

The equivalent bonds, C-8a—O1 of ring C, and C-1″—O of ring E, for R = $OCH_3$ (**3**) and R = OH (**2**), did not behave as C-2—O1 and C-2—O, which were characterized as covalent polarized bonds (shared-type atomic interactions with high $\rho_b$, negative $\nabla^2\rho_b$, $|\lambda_1|/\lambda_3 > 1$, and $G_b/\rho_b < 1$), since showed characteristics of intermediate interactions (high $\rho_b$, negative $\nabla^2\rho_b$, $|\lambda_1|/\lambda_3 < 1$, and $G_b/\rho_b > 1$). We found that this behavior was typical of C—O bonds in 4*H*-pyran rings, where the C atoms also had $sp^2$ hybridization [11].

The BCP topological properties of C-8a—O1 and C-1″—O bonds were a consequence of the redistribution of charge density due to the conjugation of the O1 and O lone pairs with π-orbitals (Table 2) as in the unsubstituted compound **1**. In NBO analysis, the electronic wave functions can be interpreted in terms of a set of Lewis occupied orbitals and a set of unoccupied non-Lewis localized orbitals. Delocalization of electron density between occupied Lewis-type (bonds or lone pairs) NBO orbitals and formally unoccupied non-Lewis (anti-bonds or Rydberg) NBO orbitals accounted for stabilizing donor–acceptor interactions. We found that nonbonding molecular orbitals (lone pairs) of the substituted compounds **2** and **3** also had distinct functions according to their position relative to the neighboring aromatic rings, as shown in Table 2. The O and O1 lone pairs above the molecule plane ($1n$) are *sp*-type and are involved in interactions with the $\sigma$ system (anomeric effect), while those below the plane ($2n$) are *p*-type, which are conjugated with π-orbitals. Through the NBO analysis, we observed the same resonance effect on 2,3-dihydrobenzo-γ-pyran [11]. These conjugative and hyperconjugative interactions explained the increase in the positive Hessian eigenvalue ($\lambda_3$ curvature) at their CPs, and the distinctive features of the O1—C-8a bond *vs.* O1—C-2 (and O—C-1″ *vs.* O—C-2) mentioned above, and were associated with a higher charge concentration on C-8a and C-1″ than on C-2 (119.62 a.u. at NCP for C-8a and C-1″ *vs.* 119.54 a.u. at NCP for C-2, in CT isomers). It is worth mentioning that for **2** substituted with R = OH charge concentration was higher on C-1″ (119.621 a.u.) than on C-8a (119.620 a.u.). A Laplacian contour map of the electron density function for the ring D plane is shown in Fig. S3. There was a slight asymmetry between C-2—O1 and C-8a—O bonds and between C-2—O and C-1″—O bonds in the inner contour lines, the high values of $\nabla^2\rho_b$ were spread over the C-8a—O and C-1″—O bonding spatial regions in accordance with covalent polar intermediate interactions characterized by large values of $\lambda_3$. The same graphical behavior was observed for C-5″—O and C-3″—O bonds in both conformers with R = OH (**2**) and with R = $OCH_3$ (**3**), according to their classification as covalent intermediate interactions due to high $\rho_b$, negative $\nabla^2\rho_b$, $|\lambda_1|/\lambda_3 < 1$, and $G_b/\rho_b > 1$ (Tables S1–S3).

The C—H bonds showed $\rho_b$ values in the range of 0.276–0.283 a.u., and $\nabla^2\rho_b$ values in the range of (−0.922)–(−0.977) a.u. The C—H bonds of rings A, B and D were stronger than C-3—H and C-4—H. The weakness of the latter bonds was associated with their role as donors in hyperconjugative interactions as described for the unsubstituted compound **1** [11].

In fact, there were significant delocalizations of the C-3—H bonding orbitals towards antibonding orbitals of antiperiplanar bonds, e.g., C-2–O1/O and C-4—C-4a/C-6″ bonds, as shown in Table 3. The second order energy of the $\sigma_{C-H} \rightarrow \sigma^*_{C-O}$ transfer was higher than the energy of $\sigma_{C-H} \rightarrow \sigma^*_{C-C}$ (mean difference $\Delta_{(C-O)-(C-C)}$ = 5.20–2.61 kcal mol$^{-1}$ = 2.59 kcal mol$^{-1}$, taking into account all conformers). Moreover, when comparing similar conformers, such as $Z1_{CT}$-R = OH (**2**) with $Z1_{CT}$-R = $OCH_3$ (**3**), we found that the energy associated with $\sigma_{C-3-H} \rightarrow \sigma^*_{C-2-O}$ transfers was modulated by substituent effects, showing an increase according to R = H < R = $OCH_3$ < R = OH (Table 3). Therefore, there was an increase of electron delocalization in the same order.

The C-4—C-4a, C-4—C-6″, C-2—C-3, and C-3—C-4 bonds (rings C and E) had a slightly longer length ($\Delta$ = 0.11 Å,) than other C—C bonds as well as lower $\rho_b$ values (0.245 *vs* 0.307 as mean values),

**Table 2**
Main natural bond orbital (NBO) second-order stabilization energies, $E^{(2)}$, calculated at B3LYP/6-311++G** level of theory, for $1,2n_O$, $1,2n_{O1}$ and $\sigma_{(C-O)}$ donors. Other relevant interactions are also shown.[a]

| | | R = OH | | | | | | | | R = $OCH_3$ | | | R = H[b] | |
|---|---|---|---|---|---|---|---|---|---|---|---|---|---|---|
| Donor | Acceptor | $Z1_{CT}$ | $Z1_{CC}$ | $Z1_{TC}$ | $Z1_{TT}$ | $Z2_{CT}$ | $Z2_{CC}$ | $Z2_{TC}$ | $Z2_{TT}$ | $Z1_{CT}$ | $Z1_{CC}$ | $Z2_{CC}$ | Z1 | Z2 |
| $1n_{O1}$ | $\sigma^*_{C-8-C-8a}$ | 0.56 | 0.56 | 0.58 | 0.58 | 0.55 | 0.55 | 0.57 | 0.57 | 0.55 | 0.56 | 0.54 | 0.56 | 0.54 |
| $1n_{O1}$ | $\sigma^*_{C-4a-C-8a}$ | 7.07 | 7.09 | 7.24 | 7.22 | 7.02 | 7.05 | 7.28 | 7.25 | 7.09 | 7.10 | 7.07 | 7.15 | 7.12 |
| $2n_{O1}$ | $\pi^*_{C-4a-C-8a}$ | 25.64 | 25.84 | 26.68 | 26.46 | 25.93 | 26.15 | 25.18 | 25.00 | 25.68 | 25.87 | 26.23 | 26.3 | 26.70 |
| $1n_O$ | $\sigma^*_{C-1''-C-6''}$ | 6.73 | 6.84 | 7.01 | 6.75 | 6.95 | 6.97 | 6.83 | 6.81 | 6.58 | 6.62 | 6.74 | 7.15 | 7.11 |
| $2n_O$ | $\pi^*_{C-1''-C-6''}$ | – | – | – | – | – | – | – | – | – | – | – | 26.31 | 26.70 |
| $1n_O$ | $\sigma^*_{C-1''-C-2''}$ | 0.54 | 0.63 | 0.58 | 0.59 | 0.53 | 0.55 | 0.51 | – | 0.56 | 0.59 | 0.59 | 0.56 | 0.54 |
| $2n_O$ | $\pi^*_{C-1''-C-2''}$ | 27.38 | 26.99 | 26.13 | 26.51 | 27.77 | 27.37 | 26.02 | 26.43 | 26.35 | 26.27 | 26.66 | – | – |
| $1n_{O1}$ | $\sigma^*_{C-2-C-1'}$ | 0.83 | 0.82 | 0.79 | 0.79 | 0.81 | 0.80 | 0.67 | 0.68 | 0.81 | 0.81 | 0.79 | 0.82 | 0.79 |
| $2n_{O1}$ | $\sigma^*_{C-2-C-1'}$ | 1.19 | 1.15 | 1.20 | 1.24 | 0.91 | 0.88 | 1.46 | 1.48 | 1.21 | 1.19 | 0.85 | 1.09 | 0.75 |
| $1n_{O1}$ | $\sigma^*_{C-2-C-3}$ | 4.04 | 4.01 | 3.99 | 4.03 | 4.04 | 4.02 | 4.25 | 4.27 | 4.02 | 4.01 | 3.97 | 3.96 | 3.92 |
| $2n_{O1}$ | $\sigma^*_{C-2-C-3}$ | 1.59 | 1.61 | 1.52 | 1.50 | 1.54 | 1.55 | 0.93 | 0.93 | 1.57 | 1.58 | 1.57 | 1.67 | 1.67 |
| $2n_{O1}$ | $\sigma^*_{C-2-O}$ | 14.40 | 14.28 | 13.74 | 13.81 | 14.41 | 14.31 | 12.63 | 12.73 | 14.14 | 14.10 | 14.13 | 14.03 | 14.06 |
| $\sigma_{C-2-O1}$ | $\sigma^*_{C-8a-C-8}$ | 2.20 | 2.22 | 2.27 | 2.25 | 2.25 | 2.27 | 2.47 | 2.45 | 2.21 | 2.22 | 2.43 | 2.26 | 2.32 |
| $\sigma_{C-2-O-1}$ | $\sigma^*_{C-3-H}$ | 1.03 | 1.04 | 1.03 | 1.03 | 1.14 | 1.15 | 1.09 | 1.09 | 1.03 | 1.04 | 1.15 | 1.03 | 1.15 |
| $\sigma_{C-2-O-1}$ | $\sigma^*_{C-1'-C-6'}$ | 1.94 | 1.91 | 1.89 | 1.91 | 1.52 | 1.46 | 1.28 | 1.32 | 1.94 | 1.92 | 1.42 | 1.94 | 1.41 |
| $\sigma_{C-2-O1}$ | $\sigma^*_{C-1'-C-2'}$ | 1.96 | 1.98 | 1.96 | 1.95 | – | – | – | – | 1.95 | 1.97 | – | 1.93 | – |
| $\sigma_{C-2-O}$ | $\sigma^*_{C-1'-C-6'}$ | – | – | – | – | 1.29 | 1.35 | 1.5 | 1.46 | – | – | 1.41 | – | 1.41 |
| $\sigma_{C-2-O}$ | $\sigma^*_{C-1''-C-2''}$ | 2.42 | 2.44 | 2.14 | 2.31 | 2.53 | 2.45 | 2.29 | 2.37 | 2.41 | 2.27 | 2.45 | 2.26 | 2.32 |
| $\sigma_{C-8a-O1}$ | $\sigma^*_{C-4a-C-5}$ | 1.75 | 1.76 | 1.78 | 1.78 | 1.78 | 1.78 | 1.79 | 1.79 | 1.75 | 1.75 | 1.70 | 1.75 | 1.77 |
| $\sigma_{C-8a-O1}$ | $\sigma^*_{C-7-C-8}$ | 1.34 | 1.34 | 1.33 | 1.33 | 1.33 | 1.33 | 1.40 | 1.40 | 1.33 | 1.33 | 1.45 | 1.33 | 1.33 |
| $\sigma_{C-8a-O1}$ | $\sigma^*_{C-2-C-1'}$ | 1.17 | 1.16 | 1.11 | 1.11 | 1.02 | 1.01 | 0.82 | 0.83 | 1.16 | 1.15 | 1.01 | 1.16 | 1.02 |
| $\sigma_{C-1''-O}$ | $\sigma^*_{C-2-C-1'}$ | 1.13 | 1.15 | 1.18 | 1.22 | 1.01 | 1.00 | 1.21 | 1.21 | 1.19 | 1.18 | 1.02 | 1.16 | 1.02 |
| $\sigma_{C-1''-C-6''}$ | $\sigma^*_{C-5''-O5''}$ | 3.88 | 3.68 | 4.43 | 4.20 | 3.72 | 3.82 | 4.31 | 4.15 | 3.44 | 3.54 | 3.59 | – | – |

[a] All values are expressed in kcal $mol^{-1}$.
[b] Data obtained from Ref. [11].

**Table 3**
Selected NBO second-order stabilization energies, $E^{(2)}$, calculated at B3LYP/6-311++G** level of theory, for $\sigma_{(C-3-H)}$ and some $\sigma_{(C-C)}$ donors.[a].

| | | R = OH | | | | | | | | R = $OCH_3$ | | | R = H[b] | |
|---|---|---|---|---|---|---|---|---|---|---|---|---|---|---|
| Donor | Acceptor | $Z1_{CT}$ | $Z1_{CC}$ | $Z1_{TC}$ | $Z1_{TT}$ | $Z2_{CT}$ | $Z2_{CC}$ | $Z2_{TC}$ | $Z2_{TT}$ | $Z1_{CT}$ | $Z1_{CC}$ | $Z2_{CC}$ | Z1 | Z2 |
| $\sigma_{C-3-H}$ | $\sigma^*_{C-4-C-6''}$ | 2.65 | 2.55 | 2.26 | 2.60 | 2.57 | 2.58 | 2.64 | 2.63 | 2.55 | 2.63 | 2.57 | 2.61 | 2.64 |
| $\sigma_{C-3-H}$ | $\sigma^*_{C-2-O}$ | 5.18 | 5.16 | 5.02 | 5.03 | 5.25 | 5.24 | 4.86 | 4.88 | 5.14 | 5.13 | 5.23 | 5.13 | 5.23 |
| $\sigma_{C-3-H}$ | $\sigma^*_{C-4-C-4a}$ | 2.60 | 2.62 | 2.65 | 2.64 | 2.62 | 2.62 | 2.55 | 2.55 | 2.61 | 2.61 | 2.64 | 2.61 | 2.64 |
| $\sigma_{C-3-H}$ | $\sigma^*_{C-2-O1}$ | 5.16 | 5.14 | 5.15 | 5.16 | 5.29 | 5.29 | 5.48 | 5.48 | 5.18 | 5.17 | 5.28 | 5.13 | 5.23 |
| $\sigma_{C-2-C-1'}$ | $\sigma^*_{C-1'-C-6'}$ | 1.27 | 1.28 | 1.27 | 1.26 | 1.86 | 1.86 | 1.87 | 1.87 | 1.27 | 1.27 | 1.86 | 1.26 | 1.86 |
| $\sigma_{C-2-C-1'}$ | $\sigma^*_{C-1'-C-2'}$ | 1.25 | 1.24 | 1.23 | 1.24 | 1.73 | 1.72 | 1.74 | 1.74 | 1.25 | 1.24 | 1.73 | 1.26 | 1.72 |
| $\sigma_{C-2-C-1'}$ | $\sigma^*_{C-5'-C-6'}$ | 2.29 | 2.28 | 2.29 | 2.28 | 2.32 | 2.32 | 2.29 | 2.24 | 2.29 | 2.29 | 2.32 | 2.28 | 2.31 |
| $\sigma_{C-2-C-1'}$ | $\sigma^*_{C-2'-C-3'}$ | 2.29 | 2.30 | 2.26 | 2.27 | 2.25 | 2.24 | 2.23 | 2.30 | 2.30 | 2.31 | 2.26 | 2.28 | 2.24 |
| $\sigma_{C-5'-C-6'}$ | $\sigma^*_{C-4'-H}$ | 2.59 | 2.60 | 2.58 | 2.58 | 2.62 | 2.62 | 2.61 | 2.57 | 2.60 | 2.60 | 2.62 | 2.59 | 2.62 |
| $\sigma_{C-2'-C-3'}$ | $\sigma^*_{C-4'-H}$ | 2.59 | 2.59 | 2.59 | 2.59 | 2.58 | 2.58 | 2.57 | 2.61 | 2.60 | 2.60 | 2.58 | 2.59 | 2.57 |
| $\sigma_{C-2-C-3}$ | $\sigma^*_{C-1-C-2'}$ | 0.66 | 0.62 | 0.60 | 0.64 | 2.71 | 2.71 | 2.68 | 2.69 | 0.66 | 0.64 | 2.70 | 0.67 | 2.71 |
| $\sigma_{C-5''-C-6''}$ | $\sigma^*_{C-4-C-3}$ | 0.69 | 0.71 | 0.83 | 0.83 | 0.77 | 0.77 | 0.94 | 0.95 | 0.72 | 0.67 | 0.74 | 0.78 | 0.82 |

[a] All values are expressed in kcal $mol^{-1}$.
[b] Data obtained from Ref. [11].

lower $\nabla^2\rho_b$ values (0.560 *vs* 0.845), lower $\varepsilon$ values (0.025 *vs* 0.227), and lower $|\lambda_1|/\lambda_3$ values (1.295 *vs* 1.993, mainly due to the decrease in $\lambda_1$ value). It can be drawn the conclusion from the topological parameter values that such C—C bonds are, as expected, typical single bonds stronger than those of ethane ($\rho_b$, 0.232 a.u. in ethane at the same level of calculation). The higher values of ellipticity than that of ethane indicated an asymmetrization of electronic distribution related to charge delocalization phenomena. In fact, NBO results reported above (important delocalizations of C-3—H bonding orbitals to antibonding orbitals of antiperiplanar bonds) explained the increase in BCP ellipticity of the connecting bonds (C-2—C-3 and C-3—C-4; Table S1) and explained why those ellipticities were higher in the substituted compounds **2** and **3** than in the unsubstituted **1**. NBO analysis also showed that the mean contribution of the *p* orbitals of C-3 and C-4 to the C-2—C-3 and C-3—C-4 bonds was 72.0–74.0%, respectively, while the *p* atomic orbital contribution of the C atom to the C—C bond of ethane was 70.4%. Therefore, the electron delocalization associated with these effects could indicate a mild $\pi$-character of the C-2—C-3 and C-3—C-4 single bonds, confirming this mechanism for all structures studied and light remote effects exerted by the substituents. The bond polarization or extent of ionization was described by NBO calculations of the electron density percentage on each atom of the bond. We have previously reported that the polarization of the C-2—C-3 bond of substituted and unsubstituted ($4\alpha \rightarrow 6''$, $2\alpha \rightarrow O \rightarrow 1''$)-phenylflavans was higher than that of C-3—C-4 [11,12]. Upon comparison of $Z1_{CT}$-R = OH (**2**) and $Z1_{CT}$-R = $OCH_3$ (**3**), the C-2—C-3 polarization increased as R = H < R = $OCH_3$ < R = OH [12]. These findings are consistent with the hyperconjugative interactions described above, thus showing inductive effects assisted by hyperconjugative interactions. These results further supported slight stereoelectronic effects exerted by the substituents. Moreover, evaluation of the conformational changes due to different substituent arrangements compared to the fixed position of ring B, i.e., all Z1 structures with R = OH (**2**), the "CT" structures showed that C-2—C-3 was more polarized than that of "CC", and this bond in "CC" was more polarized than those in "TC" and "TT" structures [12].

These deep analyses of the electron distribution in C-2–C-3 and the factors that may cause changes in this region might be useful in understanding the synthesis and chemical transformations of

flavans, e.g., postulated conversion of B-type into A-type proanthocyanidins [26,27].

Taking into account the conformational space, the highest ellipticity at BCP of C-6″—C-4 bond was enhanced by substitution in the order R = $OCH_3$ < R = OH. The $\sigma''''_{C-5—C-6} \rightarrow \sigma^*_{C-4—C-3}$ mean charge transfer increased in the same order (Table 3), thus explaining this trend. The C-6″—C-4 bond connects C-5″—C-6″ and C-4—C-3, which are almost antiperiplanar.

Regardless of the substitution, the C-1′–C-2 bond linking rings B and C followed a similar behavior pattern. Both Z1 and Z2 showed $\rho_b$ values of 0.304–0.310 a.u. at BCP for the C–C bonds of rings A, B and D, with $\nabla^2\rho_b$ values in the range of (−0.817)–(−0.871) a.u., and $\varepsilon$ values of 0.200–0.279 for ring A, 0.194–0.235 for ring B, and 0.249–0.280 for ring D. The values of the first two parameters suggested that C–C interactions were similar to those of benzene, calculated at the same level, e.g., $\rho_b$, 0.308 a.u.; $\nabla^2\rho_b$, −0.854 a.u.; and $\varepsilon$, 0.200, some of which being slightly stronger. Therefore, as expected, these bonds are intermediate between single and double bonds.

The ε values suggested that the π-character of these bonds decreased on average in the order ring D > ring A > ring B > benzene, as shown in Table S1. Therefore, D should be the most reactive ring towards electrophilic aromatic substitution due to the increased availability of π-electrons, which was modified by substitution, being higher when R = OH (**2**) (R = H < R = $OCH_3$ < R = OH) (Fig. S4). For R = H (**1**), the symmetrical rings A and D had a mean $\varepsilon$ value ($\varepsilon$ 0.223) higher than that of ring B ($\varepsilon$ 0.203) [11]. The increased reactivity of the substituted ring D can be also seen in Fig. S3, where the Laplacian contour maps of electron density of the substituted (4α → 6″, 2α → O → 1″)-phenylflavan Z1-isomer for the ring A plane and ring D plane are shown.

Considering ring A, the $\sigma_{C-8a-O1} \rightarrow \sigma^*_{C-4a—C-5}$, $1n_{O1} \rightarrow \sigma^*_{C-8a—C-4a}$, and $1n_{O1} \rightarrow \sigma^*_{C-8a—C-8}$ transfers led to an increase in population of the respective antibonding acceptor orbitals, resulting in the bond elongation of C-4a—C-5 (1.397 Å), C-8—C-8a (1.397 Å), and C-8a—C-4a (1.401 Å) with respect to C-8—C-7 (1.393 Å). The $\sigma_{C-8a—O1} \rightarrow \sigma^*_{C-7—C-8}$ transfer occurred, but the energy was lower than that of the $\sigma_{C-8a—O1} \rightarrow \sigma^*_{C-4a—C-5}$ transfer (1.36 kcal $mol^{-1}$ compared with 1.75 kcal $mol^{-1}$) (Table 2). Therefore, the C-8—C-7 bond was shorter than C-8a—C-4a. There were no significant $\sigma_{C—C} \rightarrow \sigma^*_{C—C}$ transfers to C-5—C-6 and C-6—C-7 antibonding orbitals, thus explaining their shorter length. These transfers accounted for the loss of ring A symmetry with respect to benzene, and may be associated with the ellipticity values of some bonds, i.e., C-8a—C-4a showed the longest bond length and highest ellipticity (Table S1). Significant $1n_{O1} \rightarrow \sigma^*_{C-8a—C-4a}$ (7.12 kcal $mol^{-1}$ on average), and $2n_{O1} \rightarrow \pi^*_{C-8a—C-4a}$ (25.91 kcal $mol^{-1}$ on average) transfers (Table 2) may explain these features. Similar results have been reported for R = H [11], supporting a general trend in these structures despite substitution. Through these mechanisms, the O1 oxygen atom donated electron density to ring A in all conformers, resulting in an increase of charge density on C-7 and C-5 (119.620 a.u., 119.604 a.u., 119.624 a.u., 119.604 a.u., 119.622 a.u., 119.607 a.u. for C-8a, C-4a, C-5, C-6, C-7, C-8, respectively).

Ring D was also asymmetrized, thus giving rise to an increase in the bond lengths of C-5″–C-6″, C-3″–C-4″, and C-1″–C-2″ in descending order. The higher bond lengths can be explained by the resonance effects of O oxygen, and oxygen-containing substituents of ring D. In fact, by charge transfer to the respective natural antibonding orbitals, O oxygen was associated with the elongation of C-1″–C-2″ bond length, O-5″ with that of C-5″–C-6″, and O-3″ with that of C-3″–C-4″ (Table S1). Furthermore, the analysis of the electron delocalization from the O lone pairs to ring D showed that $1n_O \rightarrow \sigma^*_{C-1''—C-2}$ and $2n_O \rightarrow \pi^*_{C-1''—C-2}$ transfers were usually higher for R = OH (**2**) (0.59 kcal $mol^{-1}$ and 26.75 kcal $mol^{-1}$ on average, respectively) than for R = $OCH_3$ (**3**) (0.58 kcal $mol^{-1}$ and 26.31 kcal $mol^{-1}$ on average, respectively). Therefore, this behavior was modulated by remote substituent effects according to R = $OCH_3$ < R = OH (Table 2). Our previous results also showed higher transfers from C-3″–O and C-5″–O bonds to ring D for R = OH than for R = $OCH_3$ [12], thus explaining the higher ellipticity of C-3″–C-4″ and C-6″–C-5″ bonds reported herein, being evidence for a better charge delocalization in R = OH (**2**). Moreover, the conjugation of the 2*n* lone pairs with the π -system was also significantly higher for R = OH (**2**) than for R = $OCH_3$ (**3**). Therefore, the described conjugative and hyperconjugative transfers allowed us to understand the increase in ring D mean ellipticity shown above.

In Z1 structures, the fusion of ring B with both γ-pyran rings (rings A-C and D-E) resulted in a loss of the typical benzene symmetry, so that the C-1′–C-2′ and C-1′–C-6′ bonds (1.399 Å; Table S1) were longer than the others (1.395 Å). These bonds also showed higher ellipticity than typical aromatic bonds ($\varepsilon$ 0.200). For R = OH the mean $\varepsilon$ value was 0.206, while for R = $OCH_3$ was 0.205. The ellipticities of the other bonds ranged from 0.199 to 0.202. NBO analysis showed that there was a substantial charge transfer from the C-2–C-1′ bonding orbital to C-1′–C-2′ and C-1′–C-6′ antibonding orbitals (Table 3). Moreover, transfers from C-2–O and C-2–O1 bonding orbitals to the same C-1′–C-2′ and C-1′–C-6′ antibonding orbitals (Table 2) were found. These charge transfers justify the higher bond lengths of C-1′–C-2′ and C-1′–C-6′ bonds. Energy values were important for transfers from the $\sigma_{C-2-C-1'}$ orbital to the *anti* bond orbitals regarding C-2–C-1′ bond ($\sigma^*_{C-5'-C-6'}$ and $\sigma^*_{C-2'-C-3'}$), which explains the increase in C-1′–C-2′ and C-1′–C-6′ ellipticities at CPs. We found first-related charge transfers with charge delocalization from C-2–C-1′ bonding orbital, which were $n_{O,O1} \rightarrow \sigma^*_{C-2-C-1'}$ and $\sigma_{C-8a-O1,C-1''—O} \rightarrow \sigma^*_{C-2-C-1'}$ (Table 2 and Fig. 3b). We also found first-related charge transfers with charge delocalization from C-2–O1 and C-2–O bonding orbitals, which were $\sigma^*_{C-1''-C2'',\ C-3-Ha} \rightarrow \sigma^*_{C-2-O1}$ and $\sigma^*_{C-8-C8a,\ C-3-Hb} \rightarrow \sigma^*_{C-2-O}$ (Table 3 and Fig. 3b). Moreover, we found second-related charge transfers, $\sigma_{C4a-C-5,\ C-7—C8} \rightarrow \sigma^*_{C-8a-O1}$ and $\sigma_{C-5''-C-6'',C-2''—C-3''} \rightarrow \sigma^*_{C-1''-O}$ and $\sigma^*_{C-4-C6''} \rightarrow \sigma^*_{C-3-Ha}$ and $\sigma^*_{C-4-C4a} \rightarrow \sigma^*_{C-3-Hb}$ (Fig. 3c). These charge delocalization mechanisms were cooperative, and found in all compounds studied despite substitution. Interactions between rings were explained, even in non-planar systems.

Density values on C-2′ and C-3′ in Z2 (119.631 a.u. and 119.625 a.u., respectively, in CT conformer) were higher than those of Z1 conformers (119.629 a.u. and 119.624 a.u., respectively, in CT conformer), and were associated with hyperconjugative interactions between the C-2–C-3 bond and ring B. In particular, the $\sigma_{C-2-C-3} \rightarrow \sigma^*_{C-1'-C-2'}$ transfer in Z2 was an order of magnitude higher than in Z1 for any substituent (Table 3).

The mechanisms of charge delocalization aforementioned were found for all compounds studied. These mechanisms described and quantified charge delocalization effects that connected ring B with A and D through rings C and E in flavan structures. It is usually reported that ring B of flavans is independent of ring A from the viewpoint of a π-resonant system. However, according to our results there is interaction between A and B *via* specific charge delocalization mechanisms (Fig. 3).

The C-1′–C-6′ and C-1′–C-2′ bonds were more polarized in Z1 rotamers than in Z2, suggesting a higher inductive effect in Z1 than in Z2 for all substituents, as previously reported [12]. The current work focuses on the substituent effect on this behavior, therefore we compared $Z1_{CT}$ structures with R = OH and R = $OCH_3$, and found that the polarization of C-1′–C-6′ and C-1′–C-2′ increased slightly in the order R = $OCH_3$ < R = OH. Similar results were obtained for $Z1_{CC}$ structures. This finding showed a slight substituent effect on ring B. In Z2 rotamers the effect was also stronger for R = OH.

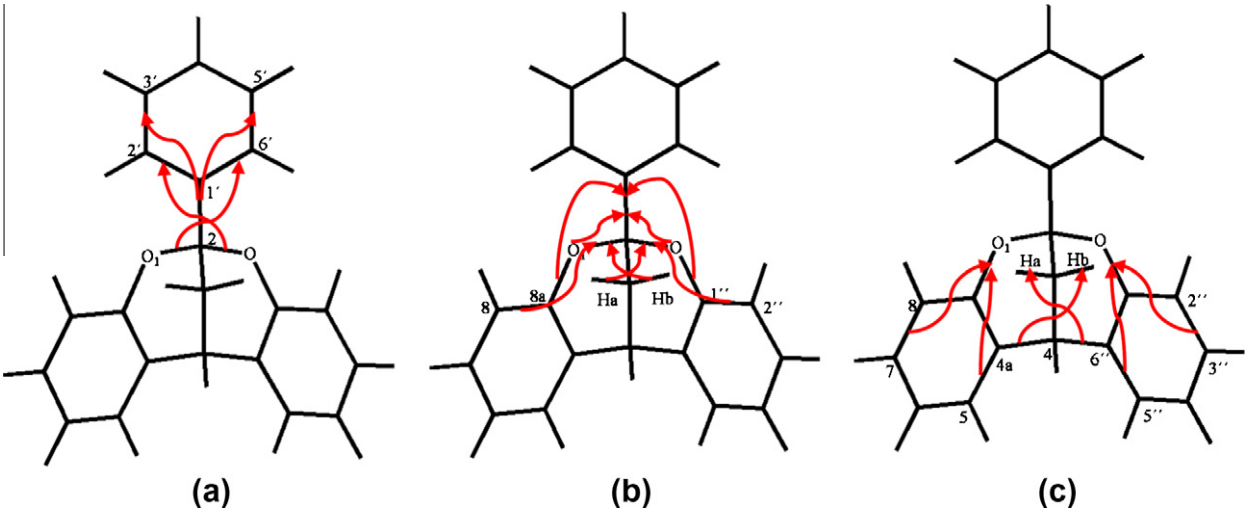


**Fig. 3.** Charge delocalization mechanisms that define the interaction between rings A, C, E and D with B ring. Direct (a), first related (b) and second related (c) charge transfers are shown.

### 3.3. NMR analysis

Calculated and experimental NMR chemical shifts ($\delta$) of the phenylflavans substituted with R = $OCH_3$ (**3**) and R = H (**1**) are shown in Fig. 4 and in Supplementary material (Table S4). Calculated values at the B3LYP/6-31G** level followed the experimental trend. Calculated NMR chemical shifts ($\delta$) of compound **2** substituted with R = OH are also shown in Fig. 4a and Table S4.

The symmetry of rings A and D observed for R = H (**1**) was lost due to substitution (**2** and **3**). The symmetry experimentally found between C-2′ and C-6′, and between C-3′ and C-5′ of ring B was also found in theoretical calculations. This symmetry was only found in the Z1 isomer (Supplementary material, Table S4), suggesting that this is the most populated rotamer in solution at room temperature, according to the relative population of these conformers shown above. In fact, the values obtained for Z2 did not follow the experimental trend.

Calculated values were similar for $Z1_{CT}$ and $Z1_{CC}$, and showed a good correlation with experimental data, except for chemical shifts of C-4″ and C-2″. The only difference between both conformers was the $CH_3$ group attached to O-3″ with respect to ring D, which freely rotated around the C-3″–O-3″ bond. The calculated C-4″ chemical shift for $Z1_{CT}$ was higher than that for $Z1_{CC}$. The chemical shift of C-2″ behaved conversely, so that the calculated C-2″ chemical shift for $Z1_{CT}$ was lower than that for $Z1_{CC}$ (Table S4). Therefore, our calculations showed shielding of C-4″ when the $CH_3$ group attached to O-3″ was in its proximity ("CC"-type arrangement), thus C-2″ being more deshielded. On the contrary, in "CT" conformer the $CH_3$ group deshielded C-4″ and shielded C-2″. Mean values agreed very well with the experimental data. This indicated the contribution of both conformers, according to their relative population and the very low energetic barriers shown above.

Therefore, NMR experimental values of the phenylflavans substituted with R = $OCH_3$ (**3**) and R = H (**1**) [11] were correlated with those obtained for the Z1 conformer, which was the most stable. This revealed that the thermodynamically most stable conformer was also the kinetically most stable one.

The effect of substituent on the chemical shifts was evaluated in the context of this work. Differences between chemical shifts of the unsubstituted compound (**1**) and those substituted with R = $OCH_3$

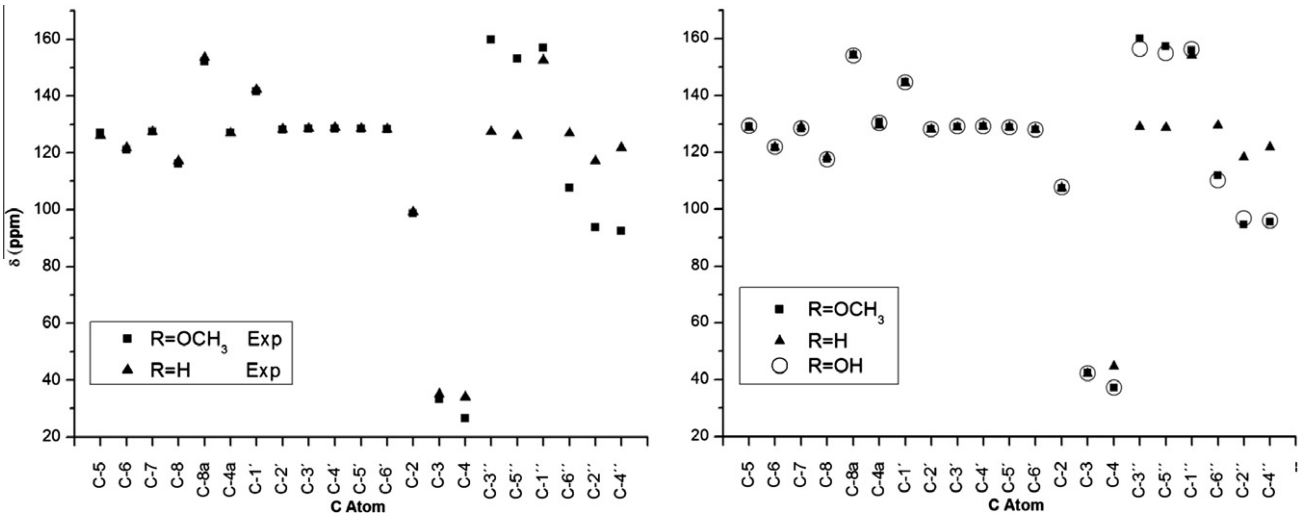


**Fig. 4.** Experimental and calculated B3LYP/6-31G** $^{13}$C-NMR chemical shifts ($\delta$) of substituted (4α → 6″, 2α → O → 1″)-phenylflavans. $\delta$ in ppm. Calculated values for $Z1_{CT}$ conformers are shown.

(**3**) and R = OH (**2**) are shown in Fig. 4b. A large shielding on C-1″, C-3″and C-5″, and a large deshielding on C-4, C-6″, C-2″and C-4″ were found. No changes were observed in other carbon atoms due to substitution. This trend was also found in the experimental values (Fig. 4a and Table S4). The substituents were strongly polar groups, therefore they introduced intramolecular electric fields, which had the effect of distorting the electron density in the rest of the molecule, mainly in ring D. Consequently, shielding constants were affected directionally, which explains the results.

### 3.4. BDE evaluation

As mentioned above, flavonoids can play a protective role by donating an H atom. Therefore, bond dissociation enthalpies (BDEs) for O-H of the OH groups attached to C-3″ and C-5″ were of particular importance in analyzing the antioxidant activity of the phenylflavans substituted with R = OH (**2**). The bond dissociation enthalpies for C–H bonds of the $OCH_3$ groups attached to C-3″ and C-5″ (**3**) were also studied with the purpose to find the structural factors and electron charge delocalization mechanisms that could be related to better BDEs values.

Gas phase BDE values that characterized the H-atom donating ability of the $Z1_{CT}$ isomers of the phenylflavans substituted with R = OH (**2**) and $OCH_3$ (**3**) were 81.79 kcal $mol^{-1}$ (in C-3″) and 81.27 kcal $mol^{-1}$ (C-5″) for R = OH (**2**), and 94.65 kcal $mol^{-1}$ (C-3″) and 94.91 kcal $mol^{-1}$ (C-5″) for R = $OCH_3$ (**3**). These BDE values for R = OH are in agreement with those previously reported for epicatechin [28]. Our results were compared with phenol as reference, and gave ΔBDE = −2.43 kcal $mol^{-1}$ (C-5″) for R = OH (**2**) (gas phase BDE for phenol at the same level of calculation was 82.70 kcal $mol^{-1}$), indicating an H-transfer easier than those calculated for tyrosol and kaempferol (ΔBDE = −0.93 kcal $mol^{-1}$ and −1.95 kcal $mol^{-1}$, respectively [14]), but worse than for epicatechin (ΔBDE = −9.17 kcal $mol^{-1}$ [14]).

The BDEs at C-3″ and C-5″ were, as expected, lower for R = OH (**2**) than for R = $OCH_3$ (**3**), which clearly confirmed that H-transfer was much easier for Z-isomers of the phenylflavans (**2**) than for (**3**). These results are consistent with previous experimental reports, showing that the OH groups have a substantial effect on the molecule, playing a positive role in antioxidant activities [5].

Moreover, we have previously reported [12] the occurrence of O-5″···H–C-5 hydrogen bond in this compound (see Fig. S5). This interaction led to a weak H-5″–O-5″ bond, and consequently, a more available H-5″, and BDEs lower in C-5″ than in C-3″ for the R = OH substitution (**2**).

Selected charge transfers, and BDE values are shown in Table 4. Our results indicated specific effects of charge delocalization that may be associated with an increased free-radical scavenging ability for *Z*-isomers of the phenylflavans substituted with R = OH (**2**):

- Conjugation of the 2*n* oxygen lone pairs of substituents with the π-system of the ring D (“*i*” transfers).
- Charge transfers from both C-3″–O and C-5”–O bonding orbitals to ring D (“*ii*” transfers).
- Charge transfers $2n_O \rightarrow \pi^{*}_{C-1''-C-2}$ and $2n_{O1} \rightarrow \pi^{*}_{C-1''-C-6}$ (“*iii*” transfers).
- Charge transfers $\sigma_{C-3-Ha} \rightarrow \sigma^{*}_{C-2-O}$ and $\sigma_{C-3-Hb} \rightarrow \sigma^{*}_{C-2-O1}$ (“*iv*” transfers).
- Charge transfers $O_{3''}$–H/$O_{3''}$–$C_{3''} \rightarrow \sigma^{*}_{C-3''-C-4''}$ and $O_{5''}$–H/$O_{5''}$–$C_{5''} \rightarrow \sigma^{*}_{C-5''-C-6''}$ (“*v*” transfers).

All of them (*i*–*v*) were more effective in the conformers of the compound substituted with R = OH (**2**) than in those with R = $OCH_3$ (**3**). Therefore, a better electron delocalization was found by the substitution with R = OH. Consequently, the structural features related to this delocalization will be useful to stabilize the radical A·, which is the product of the rapid H-atom transfer reaction.

**Table 4**
Selected NBO second-order stabilization energies, $E^{(2)}$, calculated at B3LYP/6-311++G** level of theory. BDE and adiabatic IP values are also shown.[a,b]

| Transfer | Donor | Acceptor | R = OH | R = $OCH_3$ |
|---|---|---|---|---|
| i | $2n_{O3'}$ | $\pi^{*}_{C-3''-C-4'}$ | 54.67 | 54.63 |
| | $2n_{O5''}$ | $\pi^{*}_{C-5''-C-6''}$ | | |
| ii | $\sigma_{C3''-O3''}$ | $\sigma^{*}_{C-4''-C-5''}$ | 8.00 | 7.38 |
| | | $\sigma^{*}_{C-2''-C-3''}$ | | |
| | | $\sigma^{*}_{C-1''-C-2''}$ | | |
| | $\sigma_{C5''-O5''}$ | $\sigma^{*}_{C-3''-C-4''}$ | | |
| | | $\sigma^{*}_{C-4''-C-5''}$ | | |
| | | $\sigma^{*}_{C-1''-C-6''}$ | | |
| | | $\sigma^{*}_{C-5''-C-6''}$ | | |
| iii | $2n_O$ | $\pi^{*}_{C-1''-C-2''}$ | 27.38 | 26.35 |
| iv | $\sigma_{C3-Ha}$ | $\sigma^{*}_{C-2-O}$ | 10.34 | 10.32 |
| | $\sigma_{C3-Hb}$ | $\sigma^{*}_{C-2-O1}$ | | |
| v | $\sigma_{O3''-H/C3a''}$ | $\sigma^{*}_{C-3''-C-4''}$ | 9.55 | 5.78 |
| | $\sigma_{O5''-H/C5a''}$ | $\sigma^{*}_{C-5''-C-6''}$ | | |
| | | i + ii + iii + iv + v | 109.94 | 104.46 |
| | | BDE at C-3″ | 81.79 | 94.65 |
| | | BDE at C-5″ | 81.27 | 94.91 |
| vi | $\sigma_{C3a''-H}$ | $\sigma^{*}_{O3''-C-3a''}$ | – | 9.25 |
| | “ | $\sigma^{*}_{C-3''-O3''}$ | | |
| | “ | $\sigma^{*}_{O3''-C-3a''}$ | | |
| | $\sigma_{C5a''-H}$ | $\sigma^{*}_{O5''-C-5a''}$ | | |
| | “ | $\sigma^{*}_{C-5''-O-5''}$ | | |
| | “ | $\sigma^{*}_{O5''-C-5a''}$ | | |
| | | v + vi | 9.55 | 15.03 |
| | | IP (kcal/ $mol^{-1}$) | 167.75 | 152.89 |

[a] All values are expressed in kcal $mol^{-1}$.
[b] Summation of the $E^{(2)}$ corresponding to the transfers selected, are reported.

Some consequences of increasing the hyperconjugative and resonance effects (increase in charge delocalization) by R = OH substitution of Z-isomers of phenylflavans (**2**) are as follows:

- Increased mean ellipticities at BCPs of ring D.
- Slightly increased charge concentration on C-1″.
- Slightly increased C-2–C-3, C-1′–C-6′ and C-1′–C-2′ bond polarization.
- Slightly decreased electron density at carbon atoms NCPs of ring D.

### 3.5. IP evaluation

The electron donation of the $Z1_{CT}$ isomers of the substituted compounds **2** and **3** was also studied. Adiabatic IP values were 167.00 kcal $mol^{-1}$ and 152.89 kcal $mol^{-1}$ for R = OH and R = $OCH_3$, respectively. Our results were compared with phenol as reference, and gave ΔIP = −25.8 kcal $mol^{-1}$ for R = OH, and ΔIP = −39.19 kcal $mol^{-1}$ for R = $OCH_3$ (gas phase IP for phenol at the same level of calculation was 192.08 kcal $mol^{-1}$). Therefore, electron donation for R = OH (**2**) was easier than that for tyrosol, hydroxytyrosol, gallic acid, caffeic acid, epicatechin, and kaempferol (ΔIP = −10.33 kcal $mol^{-1}$, −16.98 kcal $mol^{-1}$, −2.96 kcal $mol^{-1}$, −10.90 kcal $mol^{-1}$, −21.20 kcal $mol^{-1}$ and −24.06 kcal $mol^{-1}$, respectively [14]). Considering the electron donation mechanism and the calculated IP values, compound **3** substituted with R = $OCH_3$ was the most reactive system, even better than 6-hydroxy-2,2,5,7,8-pentamethylchroman (HPMC), which is a simplified model of α-tocopherol (ΔIP = −37,15 kcal $mol^{-1}$ [14]). No experimental data were available in the literature for IP, so that the comparison between computed and experimental values was not possible.

The adiabatic IP value for R = OH (**2**) was about 14 kcal $mol^{-1}$ higher than for R = $OCH_3$ (**3**). Therefore, substitution with R = OH lowered electron donating efficiency. However, a relatively high IP value, decreasing the electron transfer rate between the antioxidant and oxygen, was considered one of the key factors helping to enhance the antioxidant potency because of reducing the prooxidative effect of the antioxidant molecule [29,30].

Charge delocalization from the $O_{3'',5''}$–H bonding orbital to the rest of the molecule by substitution with R = OH (**2**) was lower than charge transfers from $O_{3'',5''}$–$C_{3'',5''}$ and $C_{3'',5''}$–H bonding orbitals to the rest of the molecule by substitution with R = $OCH_3$ (**3**) (transfers *v* and *vi*, Table 4). These charge delocalization mechanisms are relevant in stabilizing cation radicals, which explains the lower IP value found for R = $OCH_3$ (**3**). In fact, the ellipticity values and charge density Laplacian function analysis showed the highest reactivity of ring D and higher availability of π-electrons. Moreover, according to single-electron transfer (SET), one electron is removed from the HOMO of the parent molecule giving rise to the cation radical. HOMO of the parent molecule and its cation radical form are shown in Fig. S6. Our results showed that electron donation mainly affected ring D, thus indicating the relevance of electron delocalization from the substituents to ring D (transfers *v* and *vi* in Table 4) in the energy stabilization of the parent perturbed structure (cation radical) in the SET mechanism.

Although it is known that the best antioxidants show low IP values, an alternative mechanism for free radical scavenging has been reported [31,32], which states that antiradicals might act either donating or accepting electrons. Therefore, to understand the antiradical capacity of different molecules, it is important to study the electron transfer process, also taking into account their ability to accept electrons. For this purpose, it is necessary to assess the electron affinity (EA).

Vertical IP and EA were used to classify any substance regarding its electron donor–acceptor ability. Electron acceptance and electron donation indexes were defined using fluor and sodium as references, thus leading to the useful donator-acceptor map [33,34]. Electron acceptance index can be defined by RIP = $IP_{AH}/IP_{Na}$ and electron donation index by REA = $EA_{AH}/EA_F$, where $IP_{AH}$ and $EA_{AH}$ are the IP and EA of the antioxidant molecule. At B3LYP/6-31G** level of calculation we found RIP = 1.387 and REA = 0.360 for compound **2,** and RIP = 1.353 and REA = 0.364 for compound **3**. Therefore, our calculations show that the substitution with R = $OCH_3$ is better electron donor and slightly better electron acceptor than R = OH, because **3** has a lower IP and a slightly higher EA than **2**. Therefore, if the electron transfer mechanism is the important reaction for neutralizing free radicals, our results indicate, through a donator-acceptor map analysis, that **3** would be a better antiradical compound than **2**.

## 4. Conclusions

The resonance effects of O and O1 oxygen, and oxygen of ring D substituents explain the ring D asymmetrization of the substituted phenylflavans (similar to ring A of catechins and epicatechins). Conjugative and hyperconjugative stereoelectronic interactions described, suggest a higher reactivity of ring D. We also conclude that in flavans, even when they are nonplanar structures, the ring B is not independent of ring A, and specific charge delocalization mechanisms define the interaction between A, D and B rings in substituted phenylflavans **2** and **3**.

The theoretical NMR chemical shifts showed that at the level of calculation employed experimental trends were reproduced satisfactorily, and some charge delocalization mechanisms underlying magnetic trends could be explained. The effect of substituent was evaluated, showing a directional influence on the shielding constants.

Our results showed an enhanced free radical scavenging ability by donating an H atom for *Z*-isomers of **2** that can be related to specific charge delocalization effects. We also concluded that there are structural and electronic consequences of those increased hyperconjugative and resonance effects (increased charge delocalization) for R = OH substitution of Z-isomers of phenylflavans (**2**). Consequently, the charge delocalization mechanisms, and structural and electronic features aforementioned were suggested as significant in the enhancement of the free radical scavenging ability for R = OH substitution (**2**), and other related structures such as A-type proanthocyanidins.

Furthermore, we concluded that the enhanced antiradical activity by electron transfer can be related to electron donation affecting primarily the ring D, the electron delocalization of ring D substituents being important in stabilizing the structure of the parent perturbed structure (cation radical). Moreover, the calculation of IPs and EAs was useful for a qualitative comparison between the substances studied, thus showing that substitution with R = $OCH_3$ would lead to a better antiradical compound than with R = OH, if we are to assess the antiradical activity via electron transfer.

Our results also allow us to conclude that the enhanced energy stabilization of the cation radical or the radical generated in the free radical scavenging process could be predicted on the basis of higher resonance and other charge delocalization effects found in the corresponding AH.

We are following a program that focuses on factors that can be associated with antioxidant properties, and also those important in understanding the processes of biosynthesis, oligomerization and polymerization of flavans, through an analysis by stepwise increase in complexity. The analysis of the charge delocalization in the radicals $A^{\cdot}$ and cation radicals $AH^{\cdot+}$, substitution with R′ = R = H, OH and $OCH_3$ and the free-radical scavenging capacity in various solvents is in progress.

## Acknowledgments

Thanks are due to Agencia de Promoción Científica y Tecnológica Argentina (MINCYT), CONICET, Universidad Nacional de La Plata and Universidad de Buenos Aires (Argentina) for financial support. A.B.P. is a Senior Research Member of the National Research Council of Argentina (CONICET). A.H.J. is Member of the Scientific Research Career (CIC, Provincia de Buenos Aires). E.N.B. acknowledges a fellowship (IP-PRH N° 54) from Agencia de Promoción Científica y Tecnológica (Argentina) and Universidad de la Cuenca del Plata (Corrientes, Argentina). R.M.L. acknowledges Universidad de la Cuenca del Plata for facilities provided during the course of this work.

## Appendix A. Supplementary material

Supplementary data associated with this article can be found, in the online version, at http://dx.doi.org/10.1016/j.comptc.2012.11.008.

## References

[1] C. Manach, A. Scalbert, C. Morand, C. Remesy, L. Jimenez, Polyphenols: food sources and bioavailability, Am. J. Clin. Nutr. 79 (2004) 727–747.
[2] J. Hudec, D. Bakos, D. Mravec, L. Kobida, M. Burdovaa, I. Turianica, J. Hlusek, Content of phenolic compounds and free polyamines in black chokeberry (*Aronia melanocarpa*) after application of polyamine biosynthesis regulators, J. Agric. Food Chem. 54 (2006) 3625–3628.
[3] L.G. Espinosa-Alonso, A. Lygin, J.M. Windholm, M.E. Valverde, O. Parades-Lopez, Polyphenols in wild and weedy Mexican common beans (*Phaseolus vulgaris* L.), J. Agric. Food Chem. 54 (2006) 4436–4444.
[4] A. Pomilio, O. Müller, G. Schilling, K. Weinges, Zur Kenntnis der Proanthocyanidine, XXII. Über die Konstitution der Kondensationsprodukte von Phenolen mit Flavyliumsalzen, Justus Liebigs Ann. Chem. (1977) 597–601.

[5] J.M. Jeong, S.K. Kang, I.H. Lee, J.Y. Lee, H. Jung, C.H. Choi, Antioxidant and chemosensitizing effects of flavonoids with hydroxy and/or methoxy groups and structure-activity relationship, J. Pharm. Pharm. Sci. 10 (2007) 537–546.
[6] Z.Q. Liu, L.P. Ma, B. Zhou, L. Yang, Z.L. Liu, Antioxidative effects of green tea polyphenols on free radical initiated and photosensitized peroxidation of human low density lipoprotein, Chem. Phys. Lipids 106 (2000) 53–63.
[7] V.V. Kedage, J.C. Tilak, G.B. Dixit, T.P.A. Devasagayam, M. Mhatre, A study of antioxidant properties of some varieties of grapes (*Vitis vinifera* L), Crit. Rev. Food Sci. Nutr. 47 (2007) 175–185.
[8] M. Pinent, C. Bladé, M.J. Salvadó, M. Blay, G. Pujadas, J. Fernandez-Larrea, L. Arola, A. Ardevol, Procyanidin effects on adipocyte-related pathologies, Crit. Rev. Food Sci. Nutr. 46 (2006) 543–550.
[9] B.H. Havsteen, The biochemistry and medical significance of the flavonoids, Pharmacol. Ther. 96 (2002) 67–202.
[10] N. Cotelle, Role of flavonoids in oxidative stress, Curr. Top. Med. Chem. 1 (2001) 569–590.
[11] R.M. Lobayan, A.H. Jubert, M.G. Vitale, A.B. Pomilio, Conformational and electronic (AIM/NBO) study of unsubstituted A-type dimeric proanthocyanidin, J. Mol. Model. 15 (2009) 537–550.
[12] E.N. Bentz, A.H. Jubert, A.B. Pomilio, R.M. Lobayan, Theoretical study of Z isomers of A-type dimeric proanthocyanidins substituted with R = H, OH and OCH3. Stability and reactivity properties, J. Mol Model. 16 (2010) 1895–1909.
[13] R.M. Lobayan, E.N. Bentz, A.H. Jubert, A.B. Pomilio, Structures and electronic properties of Z isomers of ($4\alpha \rightarrow 6''$, $2\alpha \rightarrow O \rightarrow 1''$)-phenylflavans substituted with R = H, OH and $OCH_3$ calculated in aqueous solution with PCM solvation model, J. Mol. Model. 18 (2012) 1667–1676.
[14] M. Leopoldini, T. Marino, N. Russo, M. Toscano, Antioxidant properties of phenolic compounds: H-atom versus electron transfer mechanism, J. Phys. Chem. A 108 (2004) 4916–4922.
[15] A. Pomilio, B. Ellmann, K. Künstler, G. Schilling, K. Weinges, Naturstoffe aus Arzneipflanzen, XXI. $^{13}$C-NMR-spektroskopische Untersuchungen an Flavanoiden, Justus Liebigs Ann. Chem. (1977) 588–596.
[16] M.J. Frisch, G.W. Trucks, H.B. Schlegel, G.E. Scuseria, M.A. Robb, J.R. Cheeseman, J.A. Montgomery, T. Vreven Jr., K.N. Kudin, J.C. Burant, J.M. Millam, S.S. Iyengar, J. Tomasi, V. Barone, B. Mennucci, M. Cossi, G. Scalmani, N. Rega, G.A. Petersson, H. Nakatsuji, M. Hada, M. Ehara, K. Toyota, R. Fukuda, J. Hasegawa, M. Ishida, T. Nakajima, Y. Honda, O. Kitao, H. Nakai, M. Klene, X. Li, J.E. Knox, H.P. Hratchian, J.B. Cross, C. Adamo, J. Jaramillo, R. Gomperts, R.E. Stratmann, O. Yazyev, A.J. Austin, R. Cammi, C. Pomelli, J.W. Ochterski, P.Y. Ayala, K. Morokuma, G.A. Voth, P. Salvador, J.J. Dannenberg, V.G. Zakrzewski, S. Dapprich, A.D. Daniels, M.C. Strain, O. Farkas, D.K. Malick, A.D. Rabuck, K. Raghavachari, J.B. Foresman, J.V. Ortiz, Q. Cui, A.G. Baboul, S. Clifford, J. Cioslowski, B.B. Stefanov, G. Liu, A. Liashenko, P. Piskorz, I. Komaromi, R.L. Martin, D.J. Fox, T. Keith, M.A. Al- Laham, C.Y. Peng, A. Nanayakkara, M. Challacombe, P.M.W. Gill, B. Johnson, W. Chen, M.W. Wong, C. Gonzalez, J.A. Pople, Gaussian 03, Revision B.02, Gaussian, Inc. Pittsburgh PA, 2003.
[17] A.D. Becke, Density-functional thermochemistry. III. The role of exact exchange, J. Chem. Phys. 98 (1993) 5648–5652.
[18] C. Lee, W. Yang, R.G. Parr, Development of the Colle-Salvetti correlation energy formula into a functional of the electron density, Phys. Rev. B 37 (1988) 785–789.
[19] J. Zhang, F. Du, B. Peng, R. Lu, H. Gao, Z. Zhou, Structure, electronic properties, and radical scavenging mechanisms of daidzein, genistein, formononetin, and biochanin A: a density functional study, J. Mol. Struct. Theochem. 955 (2010) 1–6.
[20] Z.S. Markovic, S.V. Mentus, J.M. Dimitric Markovic, Electrochemical and density functional theory study on the reactivity of Fisetin and its radicals: implications on in vitro antioxidant activity, J. Phys. Chem. A 113 (2009) 14170–14179.
[21] E.T. Denisov, T.G. Denisova, Handbook of Antioxidant, second ed., CRC Pres LLC, Florida, 2000. pp. 83–88.
[22] H.Y. Zhang, Y.M. Sun, X.L. Wang, Substituent effects on O–H bond dissociation enthalpies and ionization potentials of catechols: A DFT study and its implications in the rational design of phenolic antioxidants and elucidation of structure–activity relationships for flavonoid antioxidants, Chem. Eur. J. 9 (2003) 502–508.
[23] F.W. Biegler-Koning, R.F.W. Bader, T.H. Tang, Calculation of the average properties of atoms in molecules. II, J. Comput. Chem. 3 (1982) 317–328.
[24] E.D. Glendening, A.E. Reed, J.E. Carpenter, F. Weinhold, NBO 3.1. Program as implemented in the Gaussian 98 package.
[25] R.F.W. Bader, Atoms in Molecules–A Quantum Theory, Oxford University Press, Oxford, 1995.
[26] D. Ferreira, D. Slade, Oligomeric proanthocyanidins: naturally occurring O-heterocycles, Nat. Prod. Rep. 19 (2002) 517–541.
[27] R.A. Dixon, D. Xie, S.B. Sharma, Proanthocyanidins – a final frontier in flavonoid research?, New Phytolog 165 (2005) 9–28.
[28] A.M. Mendoza Wilson, G.D. Avila Quezada, R.R. Baladrán Quintana, D. Glossman Mitnik, S. Ruiz-Cruz, Characterization of the semiquinones and uinines of (−)-epicatechin by means of computational chemistry, J. Mol. Struct. Theochem 897 (2009) 6–11.
[29] J.S. Wright, E.R. Johnson, G.A. Dilabio, Predicting the activity of phenolic antioxidants: theoretical method, analysis of substituent effects, and application to major families of antioxidants, J. Am. Chem. Soc. 123 (2001) 1173–1183.
[30] D.A. Pratt, G.A. Di Labio, G. Brigati, G.F. Pedulli, L. Valgimigli, 5-Pyrimidinols: novel chain-breaking antioxidants more effective than phenols, J. Am. Chem. Soc. 123 (2001) 4625–4626.
[31] A. Martinez, M.A. Rodriguez-Girones, A. Barbosa, M. Costas, Donator acceptor map for carotenoides, melatonin and vitamins, Phys. Chem. A 112 (2008) 9037–9042.
[32] A. Galano, R. Vargas, A. Martinez, Carotenoids can act as antioxidants by oxidizing the superoxide radical anion, Phys. Chem. Chem. Phys. 12 (2010) 193–200.
[33] A. Martinez, R. Vargas, A. Galano, What is important to prevent oxidative stress? A theoretical study on electron-transfer reactions between carotenoids and free radicals, J. Phys. Chem. B 113 (2009) 12113–12120.
[34] A. Martinez, Donator acceptor map of psittacofulvins ans anthocyanins: are they good antioxidant substances?, J Phys. Chem. B 113 (2009) 4915–4921.